Green Chemistry

PAPER

View Article Online
View Journal | View Issue

Check for updates

Cite this: *Green Chem.*, 2023, **25**, 2681

# Electrochemical dual α,β-C(sp$^3$)–H functionalization of cyclic *N*-aryl amines†

Tian Feng,[a] Zile Zhu,[a] Dongmei Zhang,[b] Siyi Wang,[a] Ruopu Li,[a] Zhaolin Zhu,[a] Xinxing Zhang *[b] and Youai Qiu *[a]

Received 31st January 2023,
Accepted 5th March 2023

DOI: 10.1039/d3gc00344b

rsc.li/greenchem

Herein, a straightforward and efficient route for the construction of dual α,β-C(sp$^3$)–H functionalized cyclic *N*-aryl amines using a combination of electrocatalysis and iron catalysis is disclosed. This method is achieved by multiple single electron oxidations and is carried out in an operationally simple manner with high chemo- and site-selectivity, setting the stage for the challenging multiple site selective C–H functionalization. The mechanism is supported by a variety of experimental probes and theoretical investigations, including cyclic voltammetry tests, a bipolar ultramicroelectrode (BUME) methodology combined with nano-electrospray ionization mass spectrometry, and density functional theory calculations.

Published on 09 maart 2023. Downloaded on 13/10/2025 18:40:56.

## Introduction

Electrocatalysis has gained popularity over the past few years as an alternative and environmentally-friendly method for sustainable transformations in modern organic synthesis. It benefits from bypassing the use of stoichiometric oxidants or reductants through efficient electron transfer[1] and has been applied to C–H activation,[2] alkene functionalization,[3] C–H oxidation,[4] cross-coupling reactions,[5] and others.[6] Among which, electro-oxidative C(sp$^3$)–H bond functionalization attracts much attention because the C(sp$^3$)–H bond is one of the most ubiquitous motifs in organic molecules, including the benzylic C(sp$^3$)–H bond,[4e,7] the allylic C(sp$^3$)–H bond,[2g,4b,8] the C(sp$^3$)–H bond adjacent to an X (X = N, O, S) atom[6f,9] represented by Shono oxidation,[10] and even the inert C(sp$^3$)–H bond (Fig. 1a)[2c,4c,11] Despite the significant progress in this field, the vast majority of such methods have mainly focused on the transformation of the single C(sp$^3$)–H bond, whereas many synthetic targets require the transformation of multiple C–H bonds which have been far elusive. One of the major challenges of such reactions is that the installation of one functional group is inclined to deactivate the surrounding C–H bonds. Hence, the development of simultaneous electrochemical methodologies for direct, efficient, and selective multiple C–H functionalization in a greener, more general, and economic way, facilitating potential practical applications, is still scarce and highly desirable yet challenging.[12] Notably, Lambert and co-workers reported an elegant electrophotocatalytic diamination of vicinal C(sp$^3$)–H bonds by successive Ritter-type aminations,[13] using a combination of light and electrical energy,[14] and this strategy was also further success-

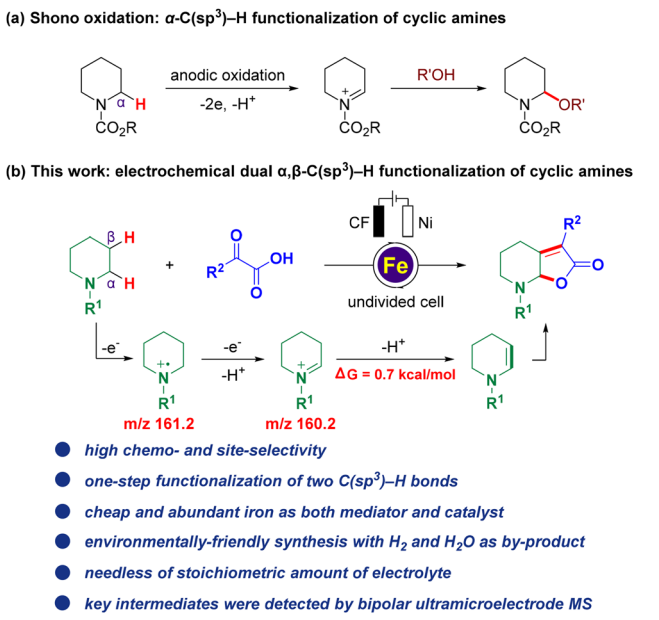


**Fig. 1** Background and current work. (a) Shono oxidation: α-C(sp$^3$)–H functionalization of cyclic amines. (b) Electrochemical dual α,β-C(sp$^3$)–H functionalization (this work).

[a]*State Key Laboratory and Institute of Elemento-Organic Chemistry, Frontiers Science Center for New Organic Matter, College of Chemistry, Nankai University, 94 Weijin Road, Tianjin, 300071, China. E-mail: qiuyouai@nankai.edu.cn*
[b]*Key Laboratory of Advanced Energy Materials Chemistry (Ministry of Education), Renewable Energy Conversion and Storage Center (RECAST), Frontiers Science Center for New Organic Matter, College of Chemistry, Nankai University, 94 Weijin Road, Tianjin, 300071, China. E-mail: Zhangxx@nankai.edu.cn*

†Electronic supplementary information (ESI) available. CCDC 2218711. For ESI and crystallographic data in CIF or other electronic format see DOI: https://doi.org/10.1039/d3gc00344b

Published on 09 maart 2023. Downloaded on 13/10/2025 18:40:56.

fully applied to the oxygenation of multiple adjacent C($sp^3$)–H bonds,[15] which are elegant examples of synthesizing multi-functionalized compounds by electrophotocatalysis with the potential for further applications.

With our continuous interest in the electrochemical C–H functionalization of cyclic amines[16] and sustainable electrochemical transformation,[17] herein, we report the first iron-catalyzed electrochemical dual α,β-C($sp^3$)–H functionalization of cyclic amines (Fig. 1b). Notable features include: (a) high chemo- and site-selectivity, (b) one-step functionalization of vicinal C($sp^3$)–H bonds, (c) an inexpensive and Earth-abundant iron complex used as both a mediator and catalyst, (d) environmentally-friendly synthesis with $H_2$ and $H_2O$ as by-products and (e) non-requirement of stoichiometric amounts of the electrolyte.

## Results and discussion

### Optimization of electrochemical dual C($sp^3$)–H functionalization

We began our investigation by employing *N*-phenyl piperidine **1** and 2-oxo-2-phenylacetic acid **2** as model substrates for the initial optimization of the envisioned transformation. To our delight, the desired dual C($sp^3$)–H functionalized product **3** was obtained in 80% yield with constant current electrolysis selectively performed in the presence of a catalytic amount of the iron catalyst (Fe(phen)$Cl_3$ (10 mol%)) with cheap carbon felt (CF, price of CF: 25 dollars per $m^2$, and the CF could also be reused.) being employed as the anode and a nickel plate as the cathode (Table 1, entry 1). To further optimize this reaction, several reaction parameters were examined. Firstly, control experiments showed that only a trace amount of the dual functionalized product was obtained in the absence of Fe(phen)$Cl_3$, which demonstrated the crucial role of the iron catalyst (Table 1, entry 2). Interestingly, 7% of **3** was obtained without electricity, and it was considered that the Fe(III) complex could undergo a single electron transfer (SET) with **1** (Table 1, entry 3). Using $FeCl_3$ (10 mol%) and 1,10-phenanthroline (10 mol%) in place of Fe(phen)$Cl_3$ resulted in a lower yield of **3** (59%) (Table 1, entry 4), and in the absence of 1,10-phenanthroline, the yield of the product harshly decreased to 44% with a considerable amount of the starting material remaining, which demonstrated the significant role of the ligand (Table 1, entry 5). Different valences of iron catalysts were also investigated, such as Fe(phen)$Cl_2$, which gave the product in a lower yield (58%) (Table 1, entry 6). Next, considering that the iron catalyst could also act as a Lewis acid in this transformation, we explored other commonly used Lewis acids such as $ZnCl_2$, $CuCl_2$, and $B(C_6F_5)_3$, and the results showed a much lower efficiency (Table 1, entry 7) or even complete impediment of the reaction (Table 1, entry 8). Using a graphite felt anode instead of carbon felt afforded the desired product in 56% (Table 1, entry 9). Replacing the Ni plate with a Pt plate as the cathode furnished the product with a slight decrease in the yield (Table 1, entry 10), and when a larger specific surface area Ni foam was also used as the cathode, it resulted in only 38% yield of **3** (Table 1, entry 11). Next, we investigated the influence of the constant current and temperature, and the results showed that a higher current led to a lower yield of **3** (54%) possibly due to overoxidation (Table 1, entry 12). The reaction worked well at a lower temperature (50 °C) although in a slightly lower yield (66%, Table 1, entry 13), and 35% yield of **3** was obtained at room temperature (Table 1, entry 14).

Table 1 Screening of the reaction conditions[a]

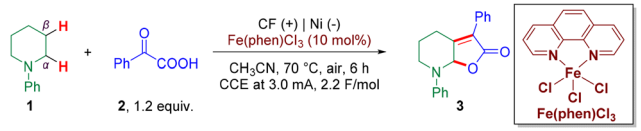


| Entry | Variation | Yield[b]/% |
|---|---|---|
| **1** | **None** | **80** |
| 2 | No Fe(phen)$Cl_3$ | Trace |
| 3 | No electricity | 7 |
| 4 | $FeCl_3$ (10 mol%) + 1,10-phen (10 mol%) | 59 |
| 5 | w/o 1,10-phen | 44 |
| 6 | Fe(phen)$Cl_2$ | 58 |
| 7 | $ZnCl_2$ or $CuCl_2$ | 26 or 33 |
| 8 | $B(C_6F_5)_3$ | — |
| 9 | GF (+) | 56 |
| 10 | Pt (−) | 73 |
| 11 | Ni foam (−) | 38 |
| 12 | 5.0 mA | 54 |
| 13 | 50 °C | 66 |
| 14 | RT | 35 |

[a] Reaction conditions: undivided cell, carbon felt (CF) anode, nickel plate cathode, constant current = 3.0 mA, *N*-phenyl piperidine **1** (0.3 mmol), 2-oxo-2-phenylacetic acid **2** (0.36 mmol, 1.2 equiv.), Fe(phen)$Cl_3$ (10 mol%), $CH_3CN$ (5.0 mL), 70 °C, 6 h. [b] Yield of the isolated product. GF = graphite felt. RT = room temperature.

### Substrate scope

Encouraged by the successful optimization of the reaction conditions, we explored the generality of this electrochemical dual C($sp^3$)–H functionalization on various cyclic *N*-aryl amines and aryl keto acids (Fig. 2). Firstly, a diverse range of *N*-aryl piperidines bearing different electron donating groups (EDGs) or electron withdrawing groups (EWGs) were screened, which all worked well to afford the corresponding products in moderate to good yields (**4–13**), and no obvious electronic affect was observed. Other aryl motifs, including naphthalene (Np) and dihydrobenzofuran, were all well tolerated and gave the corresponding products in moderate yields (**14**, **15**). Substrates bearing different substituents on the piperidine motif such as 2-Me, 3-Me, 4-Me, or even a potentially sensitive ester group at the 4-position all worked smoothly and generated the corresponding products with a diastereomeric ratio of 3 : 1 and 1.67 : 1 for **16** and **17**, respectively. Remarkably, 4-Me and 4-$CO_2$Et substituted piperidine substrates could furnish the corresponding products in high levels of stereoselectivity (**18**, **19**), and the configuration of **19** was verified by X-ray analysis. To our

 This journal is © The Royal Society of Chemistry 2023

Published on 09 maart 2023. Downloaded on 13/10/2025 18:40:56.

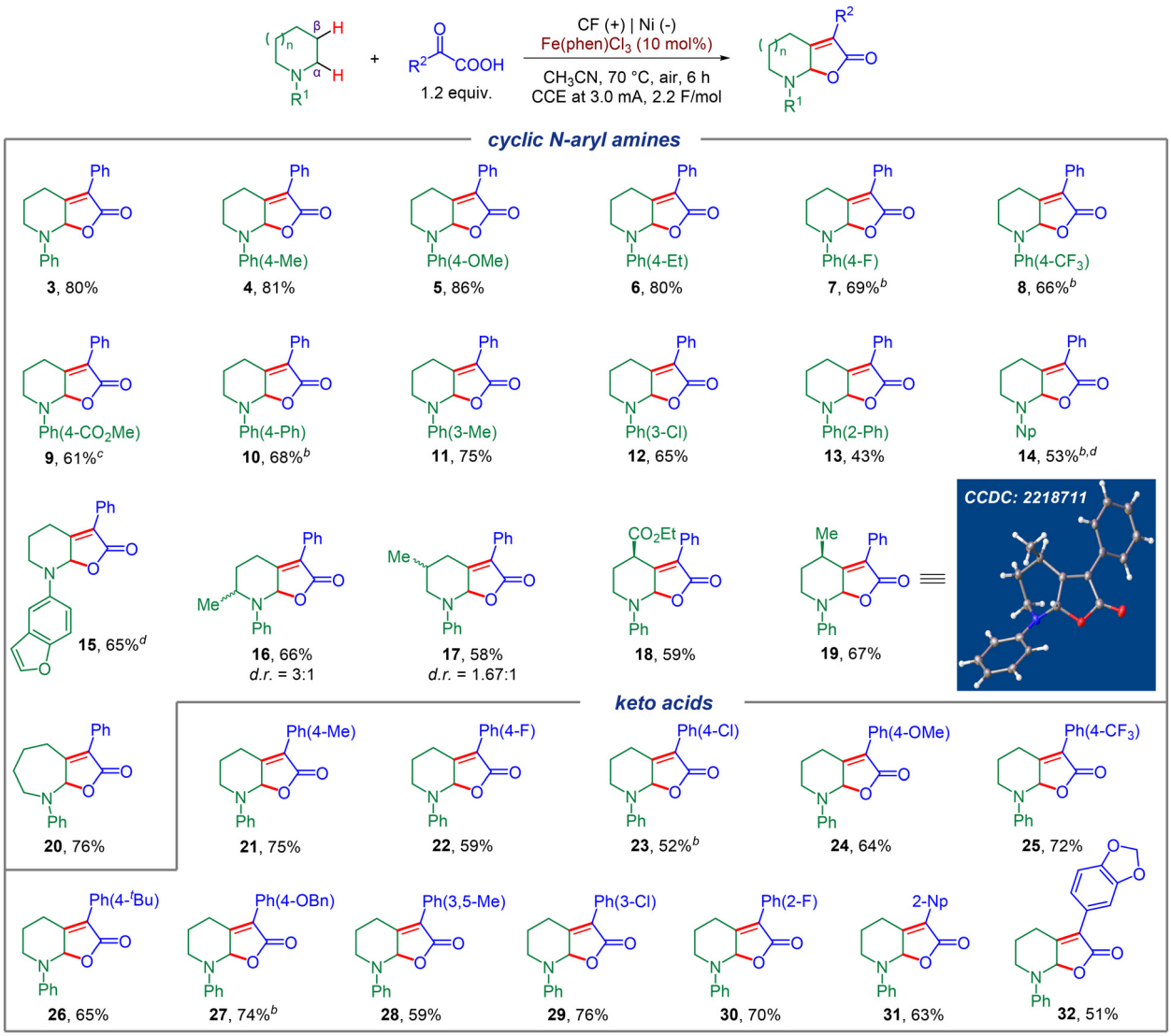


**Fig. 2** Scope of the electrochemical dual C($sp^3$)–H functionalization. Reaction conditions: carbon felt anode, Ni plate cathode, cyclic *N*-aryl amines (0.3 mmol), aryl keto acid (0.36 mmol, 1.2 equiv.), Fe(phen)$Cl_3$ (10 mol%), $CH_3CN$ (5.0 mL), constant current = 3.0 mA, 70 °C, air, 6 h. [a]5 mA. [b]7 mA. [c]24 h.

delight, substrates with different ring sizes of cyclic *N*-phenyl amines, also successfully led to the formation of the corresponding seven-membered product with good efficiency (for example, **20**). Next, we focused on the scope of the α-aryl keto acid component. Both EDGs and EWGs at the *ortho*-, *meta*- or *para*-position of the benzene ring could furnish the corresponding desired products in moderate to good yields (**21–30**), and no obvious electronic effect was observed. In addition, this electrochemical C($sp^3$)–H dual functionalization was also compatible with other aromatic motifs such as 2-Np and MDB (1,2-methylenedioxybenzene) substituted keto acids, furnishing **31** and **32** in good yields.

We next investigated the application of this electrochemical dual C($sp^3$)–H functionalization for late-stage modification (Fig. 3). To our delight, a variety of complex compounds were suitable substrates. Carbohydrates such as D-Galactose (**33**) could furnish the corresponding dual functionalization product in 58% yield with a diastereomeric ratio of 1 : 1 (see the ESI for details†). Moreover, different configurations of D-mannofuranose reacted smoothly to generate products **34** and **35** in 53% and 61% yields, respectively. Furthermore, the use of natural product derivatives such as DL-isoborneol and DL-menthol furnished the desired products with good efficiency (**36**, **37**, and **38**, respectively). Notably, a potentially sensitive ester group was well tolerated and gave the corresponding product **38** in 68% yield (dr = 1 : 1). The unique ability of this dual functionalization strategy was also highlighted by the modification of derivatives of α-amino acids. To this end, natural amino acid derivatives of L-phenylalanine bearing a piperidine motif were investigated and the corresponding products with α-phenyl (4-H, 4-OMe) keto acids were obtained in good yields (**39**, **40**).

Published on 09 maart 2023. Downloaded on 13/10/2025 18:40:56.

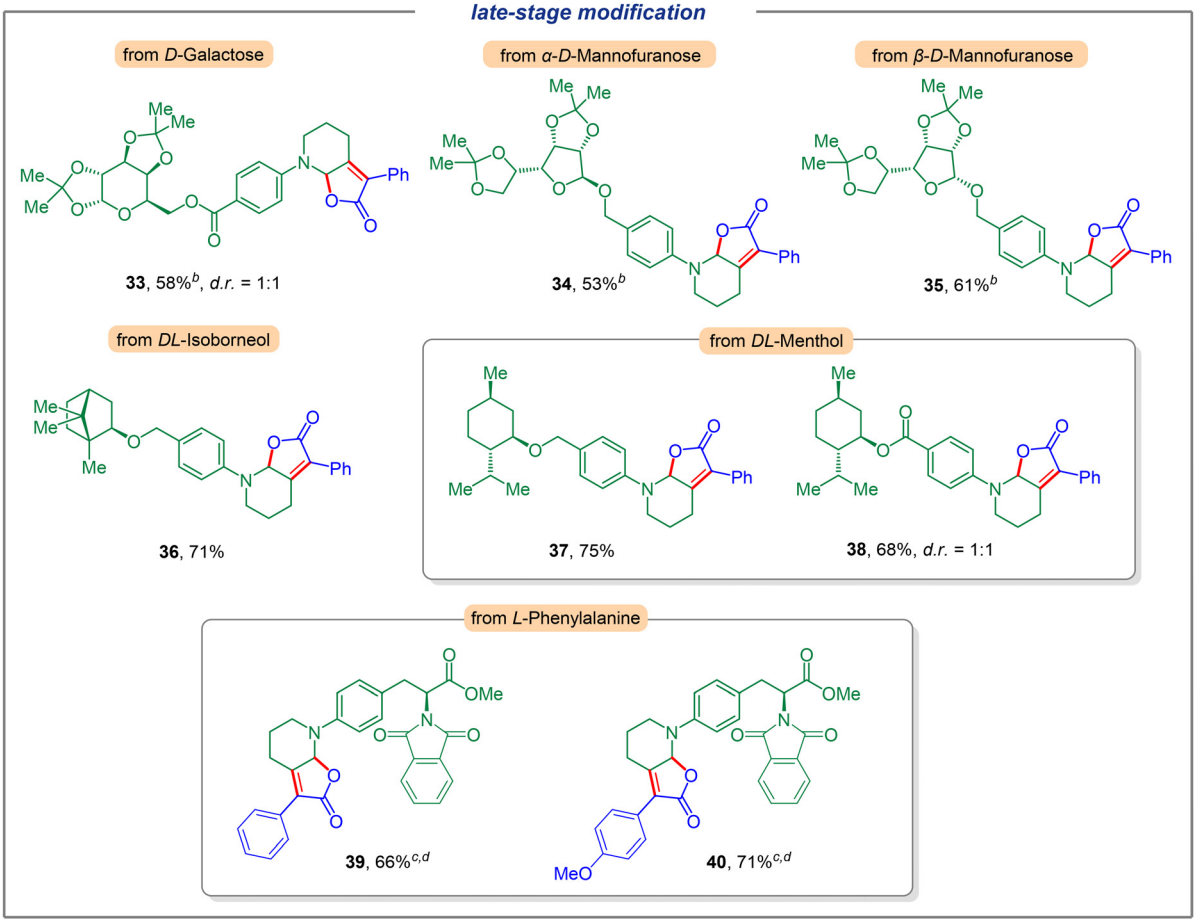


**Fig. 3** Late-stage modification. Reaction conditions: carbon felt anode, Ni plate cathode, *N*-aryl piperidine (0.3 mmol), aryl keto acid (0.36 mmol, 1.2 equiv.), Fe(phen)$Cl_3$ (10 mol%), $CH_3CN$ (5.0 mL), constant current = 3.0 mA, 70 °C, air, 6 h. [a]5 mA. [b]7 mA. [c]24 h.

## Mechanistic studies

To further illustrate the synthetic utility of this method, we carried out a gram-scale preparation of the product. As a result, the reaction of *N*-phenyl piperidine **1** (10 mmol, 1.61 g) with 2-oxo-2-phenylacetic acid **2** (12 mmol, 1.2 equiv.) under a constant current at 50 mA, furnished product **3** in 61% isolated yield (1.78 g) after 12 hours (Fig. 4A). Notably, the catalyst loading could be further reduced to 3 mol%.

Next, we sought to demonstrate the role of the iron catalyst. Firstly, we synthesized and isolated Fe complex **41** by treating 2-oxo-2-phenylacetic acid **2** with Fe(phen)$Cl_3$ in $CH_3CN$ at 70 °C for 3 h, according to the method of a previous report (Fig. 4B, (i)),[18] and we hypothesized that this Fe complex could furnish the transformation directly. However, it turned out that **41** could not furnish product **3** under the standard conditions (Fig. 4B, (ii)). This result revealed that Fe(phen)$Cl_3$ could not dissociate and participate in the catalytic cycle under standard conditions. The dissociation of the iron catalyst involves a chlorine anion to generate Fe(phen)$Cl_3$ from **41**, as a consequence, a catalytic amount of HCl (1.0 M, 0.2 equiv.) was added to the reaction, and the desired product **3** could be obtained in 59% yield, which supported the abovementioned hypothesis (Fig. 4B, (iii)). Next, the reaction of *N*-phenyl piperidine **1** and **41** could furnish the desired product **3** in 73% yield on introducing 1 mol% Fe(phen)$Cl_3$ (Fig. 4B, (iv)). These results support that Fe(phen)$Cl_3$ could act as both a catalyst and an electro-mediator.

In order to further understand the reaction mechanism of this electrochemical dual C($sp^3$)–H functionalization, several cyclic voltammetry (CV) tests were performed. As depicted in Fig. 4C, an irreversible oxidation peak of *N*-phenyl piperidine **1** at $E$ = 0.66 V (*vs.* $Ag/Ag^+$) was observed at a scan rate of 100 mV $s^{-1}$ (Fig. 4C (a), red line). Intriguingly, another oxidation peak of **1** at $E$ = 1.17 V (*vs.* $Ag/Ag^+$) was observed (Fig. 4C (a), green line) when the CV test was performed at a different scan rate (75 mV $s^{-1}$). We speculated that this oxidation peak could be the second oxidation of *N*-phenyl piperidine **1** according to previous reports.[19] Surprisingly, an obvious catalytic current appeared and the second oxidation peak increased distinctly from 0.49 mA to 0.75 mA in the presence of Fe(phen)$Cl_3$ (Fig. 4C (a), blue line), which demonstrated that the Fe catalyst likely participates in the second electron transfer process from the *N* radical cation to the iminium ion as an oxidative

 This journal is © The Royal Society of Chemistry 2023

Published on 09 maart 2023. Downloaded on 13/10/2025 18:40:56.

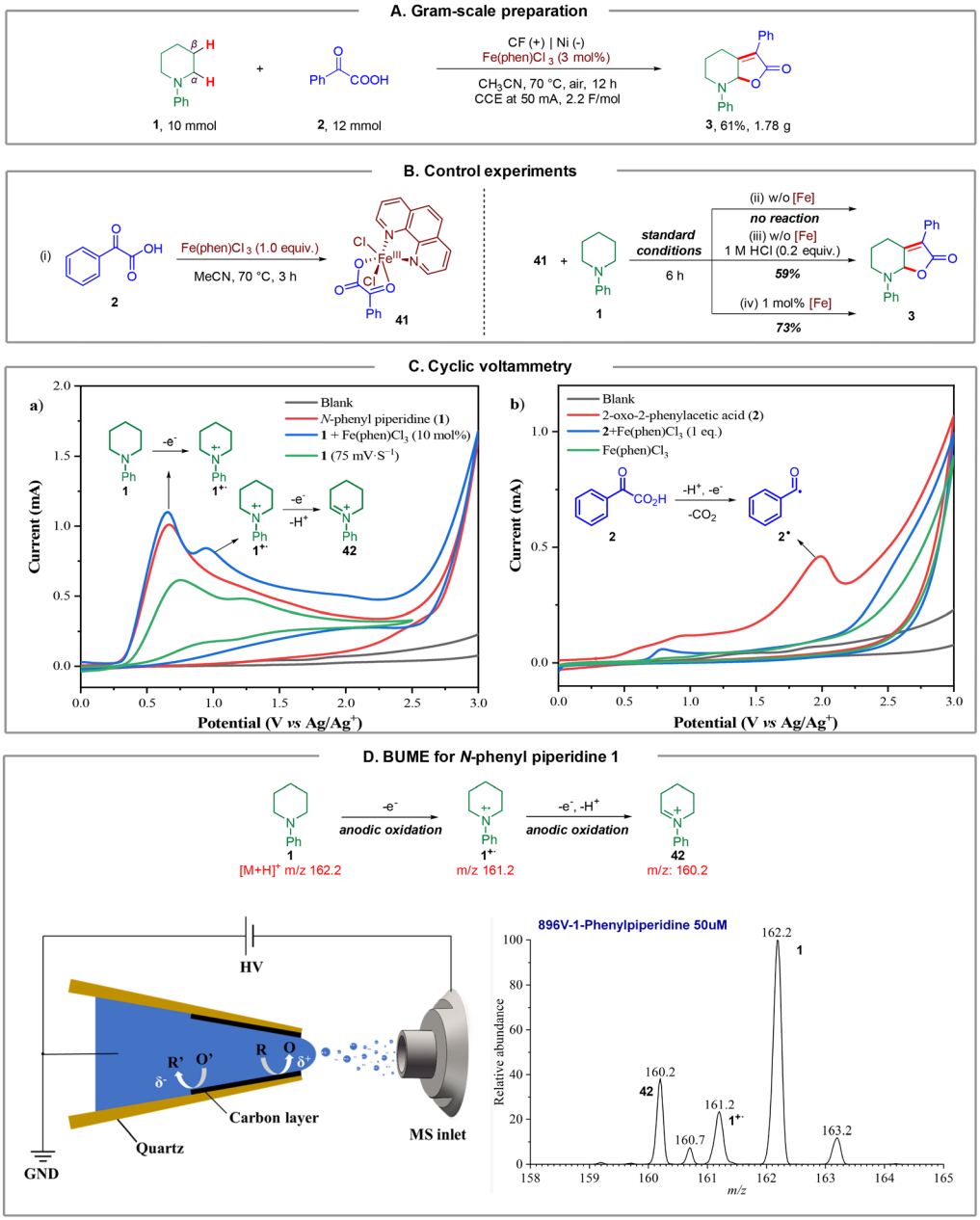


**Fig. 4** Mechanistic studies. (A) Gram-scale preparation. (B) Control experiments. (C) Cyclic voltammetry, using glass carbon as the working electrode, Pt plate as the counter electrode and $Ag/Ag^+$ as the reference electrode. ($CH_3CN$, **1** (10.0 mM), **2** (10.0 mM), $Fe(phen)Cl_3$ (1.0 mM), 0.1 M $^nBu_4NBF_4$, 100 $mVs^{-1}$). (D) BUME of the twice single electron oxidation.

mediator. In addition, 2-oxo-2-phenylacetic acid **2** exhibited an oxidation peak at $E$ = 1.99 V (*vs.* $Ag/Ag^+$) as shown in Fig. 4C (b) (red line), representing the electrochemical decarboxylation process. No peaks of $Fe(phen)Cl_3$ could be observed (Fig. 4C (b), green line) and, in sharp contrast, the oxidation peak of **2** surprisingly disappeared in the presence of 1.0 equivalent of $Fe(phen)Cl_3$ (Fig. 4C (b), blue line), which supports that the presence of $Fe(phen)Cl_3$ clearly restrained the oxidation of the keto acid and hence we consequently speculated that $Fe(phen)Cl_3$ could also prevent the keto acid from decarboxylation.

To capture and identify short-lived reactive intermediates in electrochemical reactions, a bipolar ultramicroelectrode (BUME) methodology combined with nano-electrospray ionization mass spectrometry was also developed. The fabrication of the bipolar ultramicroelectrode has been described in details previously.[20] With this method, the electrospray ionization and faradaic reaction occurred simultaneously, permitting a rapid transfer of the electrochemically generated short-lived intermediates into an LTQ-XL mass spectrometer (Thermo-Fisher, Waltham, MA) for analysis. When a positive high voltage is applied, half-reactions occur on the far end of the carbon film

Published on 09 maart 2023. Downloaded on 13/10/2025 18:40:56.

that is closer to the spray tip and the mass spectrometer inlet, facilitating the mass analysis of the oxidation products. In this experiment, a positive voltage of 896 V was applied to the Cu wire to induce a redox reaction from a BUME nanopipette filled with 50 μM *N*-phenyl piperidine **1** in acetonitrile. As a result, the *N*-phenyl piperidine radical cation $\mathbf{1}^{\bullet+}$ (*m*/*z* 161.2) was immediately captured, and subsequently, the radical cation underwent another single electron oxidation, followed by deprotonation to generate iminium **42** (*m*/*z* 160.2), which was also observed by mass spectrometry (Fig. 4D), and suggested that the radical played a key role in initiating the reaction.

Then, density functional theory (DFT) calculations ((Fig. 5, for details, please see the ESI†) were conducted. Firstly, we explored the formation of the enamine intermediate **43**. According to DFT calculations, the iminium species **42** would undergo a proton transfer with *N*-phenyl piperidine **1** to afford enamine **43** and ammonium salt **1′** which provided support for this electrolyte-free electrochemical transformation. Next, Fe(phen)$Cl_3$ was proposed as the starting species, which can be coordinated with keto acid **2** *via* ligand exchange to afford *N*-phenyl piperidinium chloride and Fe complex **Int1** located at −2.0 kcal $mol^{-1}$. Simultaneously, multiple electron oxidations of *N*-phenyl piperidine **1**, along with deprotonation generated the enamine intermediate **43**. Besides, the nitrogen radical cation $\mathbf{1}^{\bullet+}$ could also be oxidized to form **42** *via* single electron transfer by $Fe^{III}$(phen)$Cl_3$ according to the CV tests, and the subsequently generated $Fe^{II}$(phen)$Cl_2$ could be oxidized by the anode to regenerate $Fe^{III}$(phen)$Cl_3$. Then, an intermolecular nucleophilic addition occurred to form intermediate **Int3** with 2.7 kcal $mol^{-1}$ *via* the transition state **TS1** located at 15.6 kcal $mol^{-1}$, followed by intermolecular hydrogen transfers to generate the enamine intermediate **Int5** with 1.9 kcal $mol^{-1}$ (path A) by traversing **TS2** located at 17.3 kcal $mol^{-1}$, and **Int5** then needed a barrier of 14.8 kcal $mol^{-1}$ for C–O bond breakage to form the intermediate **Int6** with 13.2 kcal $mol^{-1}$. Then, a hydrogen transfer followed by ligand exchange and the subsequent dehydration assisted by **1**·HCl formed **Int9** with −0.4 kcal $mol^{-1}$ of energy. Finally, the dissociation of Fe(phen)$Cl_3$ and intramolecular nucleophilic addition gave the target product **3** by traversing the transition state **TS4** located at 1.9 kcal $mol^{-1}$. For the overall reaction, the energy span ($\delta E$) of 19.3 kcal $mol^{-1}$ indicates an effective $Fe^{III}$-catalytic process, with **TS2** as the TDTS (TOF-determining transition state), and **Int1** as the TDI (TOF-determining intermediate). In order to test the sequence of the dissociation and the dehydration process, we also conceived another plausible reaction pathway, in which the dissociation of Fe(phen)$Cl_3$ occurred before the dehydration step (path B), and it was found that the energy barrier of this process was much higher than that of path A (*via* transition state **TS3′** located at 43.7 kcal $mol^{-1}$ and **Int9′** with 31.0 kcal $mol^{-1}$). Therefore, DFT calculations supported path A as the reaction mechanism for this electrochemical dual functionalization reaction.

Based on the mechanistic studies and DFT calculations, a plausible mechanism was proposed (Fig. 6). The reaction was initiated by multiple electron and proton transfer of *N*-phenyl piperidine **1** on the anode to afford enamine **43**. Besides, the nitrogen radical cation $\mathbf{1}^{\bullet+}$ could also be oxidized to form **42** *via* single electron transfer by $Fe^{III}$(phen)$Cl_3$ according to the CV tests, and the subsequently generated $Fe^{II}$(phen)$Cl_2$ could be oxidized by the anode to regenerate $Fe^{III}$(phen)$Cl_3$. Next, Fe

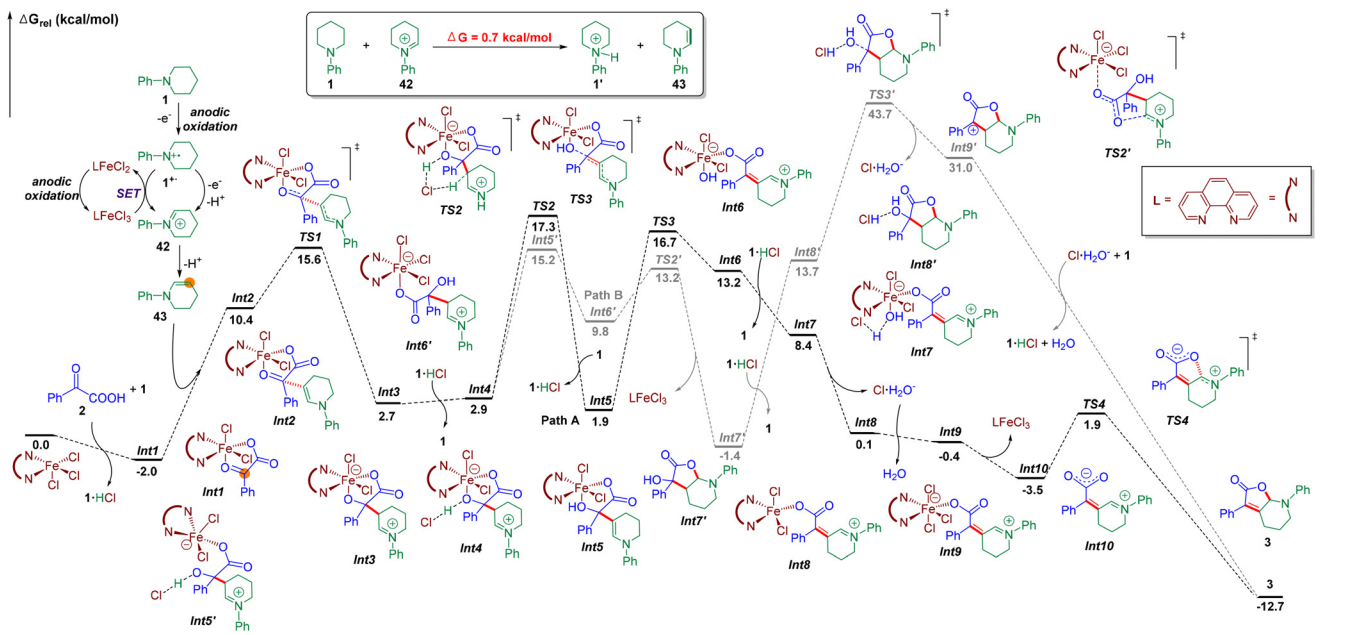


Fig. 5 DFT Calculations.


This journal is © The Royal Society of Chemistry 2023

Published on 09 maart 2023. Downloaded on 13/10/2025 18:40:56.

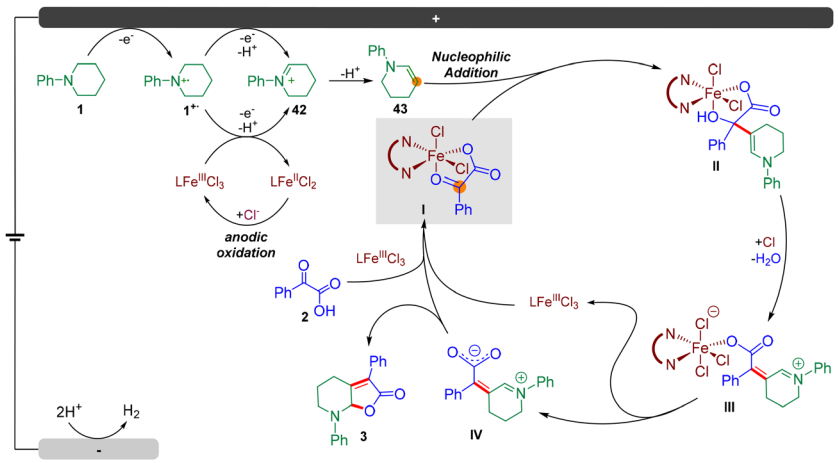


Fig. 6 The proposed catalytic cycle.

(phen)$Cl_3$ could coordinate with keto acid **2** *via* ligand exchange to afford *N*-phenyl piperidinium chloride and Fe complex **I**. Then, an intermolecular nucleophilic addition occurred, followed by intermolecular hydrogen transfers to generate the enamine intermediate **II**. Then, a hydrogen transfer followed by ligand exchange and the subsequent dehydration assisted by hydrochloric acid formed **III**. Finally, the dissociation of Fe(phen)$Cl_3$ formed intermediate **IV** and intramolecular nucleophilic addition occurred to furnish the target product **3**.

## Conclusions

In conclusion, we developed a facile, selective, and straightforward dual α,β-C($sp^3$)–H functionalization of cyclic amines with keto acids by merging electrochemistry and iron catalysis. This transformation relied on the *in situ* generation of an enamine intermediate, and the multiple single electron oxidations and deprotonations of amines, as well as the coordination between the iron catalyst and the aryl keto acid, resulted in the desired products with high chemo- and site-selectivity. The reaction proceeded smoothly in the absence of stoichiometric amounts of the electrolyte under mild conditions, possibly due to the *in situ* generated ammonium salt acting as an electrolyte. In addition, cheap carbon felt was used as the anode and Earth-abundant metal nickel was employed as the cathode. The gram-scale preparation and late-stage modification of natural product derivatives showed the potential application of the method. Specific mechanistic studies using CV tests, BUME, and DFT calculations showed consistency and support of the proposed reaction pathway. We envisioned that the potent power of this functionalization of dual $sp^3$ C–H bonds by electrocatalysis would give a potentially new perspective on the functionalization of cyclic amines and even unactivated alkyl C($sp^3$)–H bonds. Further electrochemical transformations of cyclic amines are currently underway in our laboratory.

## Author contributions

Y. Qiu, X. Zhang, and T. Feng conceived and designed the study and wrote the manuscript. T. Feng, Z. Zhu, D. Zhang, S. Wang, R. Li, Z. Zhu, X. Zhang, and Y. Qiu performed the experiments and mechanistic studies and revised the manuscript. All authors contributed to the analysis and interpretation of the data.

## Conflicts of interest

The authors declare no conflict of interest.

## Acknowledgements

Financial support from the National Key R&D Program of China (2022YFA1503200), the Fundamental Research Funds for the Central Universities (No. 63223007), the Natural Science Foundation of China (Grant No. 22188101), the Frontiers Science Center for New Organic Matter, Nankai University (Grant No. 63181206) is gratefully acknowledged. Nankai University is gratefully acknowledged and we sincerely thank Professor Qi-Lin Zhou for his generosity and key support.

## References

1 (*a*) J. Yoshida, K. Kataoka, R. Horcajada and A. Nagaki, *Chem. Rev.*, 2018, **108**, 2265–2299; (*b*) R. Francke and R. D. Little, *Chem. Soc. Rev.*, 2014, **43**, 2492–2521; (*c*) M. Yan, Y. Kawamata and P. S. Baran, *Chem. Rev.*, 2017, **117**, 13230–13319; (*d*) S. R. Waldvogel, S. Lips, M. Selt, B. Riehl and C. J. Kampf, *Chem. Rev.*, 2018, **118**, 6706–6765; (*e*) P. Xiong and H.-C. Xu, *Acc. Chem. Res.*, 2019, **52**, 3339–3350; (*f*) C. W. Anson and S. S. Stahl, *Chem. Rev.*, 2020, **120**,

Published on 09 maart 2023. Downloaded on 13/10/2025 18:40:56.

3749–3786; (*g*) L. F. T. Novaes, J.-J. Liu, Y.-F. Shen, L.-X. Lu, J. M. Meinhardt and S. Lin, *Chem. Soc. Rev.*, 2021, **50**, 7941–8002; (*h*) C. Zhu, N. W. J. Ang, T. H. Meyer, Y. Qiu and L. Ackermann, *ACS Cent. Sci.*, 2021, **7**, 415–431; (*i*) X. Cheng, A. Lei, T.-S. Mei, H.-C. Xu, K. Xu and C. Zeng, *CCS Chem.*, 2022, **4**, 1120–1152; (*j*) C. A. Malapit, M. B. Prater, J. R. Cabrera-Pardo, M. Li, T. D. Pham, T. P. McFadden, S. Blank and S. D. Minteer, *Chem. Rev.*, 2022, **122**, 3180–3218.

2 (*a*) Y. Qiu, C. Zhu, M. Stangier, J. Struwe and L. Ackermann, *CCS Chem.*, 2020, **2**, 1529–1552; (*b*) K.-J. Jiao, Y.-K. Xing, Q.-L. Yang, H. Qiu and T.-S. Mei, *Acc. Chem. Res.*, 2020, **53**, 300–310; (*c*) Q.-L. Yang, Y.-Q. Li, C. Ma, P. Fang, X.-J. Zhang and T.-S. Mei, *J. Am. Chem. Soc.*, 2017, **139**, 3293–3298; (*d*) N. Sauermann, T. H. Meyer, C. Tian and L. Ackermann, *J. Am. Chem. Soc.*, 2017, **139**, 18452–18455; (*e*) Y. Qiu, C. Tian, L. Massignan, T. Rogge and L. Ackermann, *Angew. Chem., Int. Ed.*, 2018, **57**, 5818–5822; (*f*) Q. Wang, X. Zhang, P. Wang, X. Gao, H. Zhang and A. Lei, *Chin. J. Chem.*, 2021, **39**, 143–148; (*g*) M. Chen, Z.-J. Wu, J. Song and H.-C. Xu, *Angew. Chem., Int. Ed.*, 2022, **61**, e202115954.

3 (*a*) M.-J. Luo, Q. Xiao and J.-H. Li, *Chem. Soc. Rev.*, 2022, **51**, 7206–7237; (*b*) N. Fu, G. S. Sauer, A. Saha, A. Loo and S. Lin, *Science*, 2017, **357**, 575–579; (*c*) P. Xiong, H. Long, J. Song, Y. Wang, J.-F. Li and H.-C. Xu, *J. Am. Chem. Soc.*, 2018, **140**, 16387–16391; (*d*) L. Song, N. Fu, B. G. Ernst, W. H. Lee, M. O. Frederick, R. A. DiStasio Jr. and S. Lin, *Nat. Chem.*, 2020, **12**, 747–754; (*e*) J. Ke, W. Liu, X. Zhu, X. Tan and C. He, *Angew. Chem., Int. Ed.*, 2021, **60**, 8744–8749; (*f*) D. S. Chung, S. H. Park, S.-G. Lee and H. Kim, *Chem. Sci.*, 2021, **12**, 5892–5897; (*g*) H. Huang and T. H. Lambert, *J. Am. Chem. Soc.*, 2021, **143**, 7247–7252; (*h*) X. Wu, C. N. Gannett, J. Liu, R. Zeng, L. F. T. Novaes, H. Wang, H. D. Abruña and S. Lin, *J. Am. Chem. Soc.*, 2022, **144**, 17783–17791; (*i*) S. H. Park, J. Jiang, K. Shin and H. Kim, *ACS Catal.*, 2022, **12**, 10572–10580.

4 (*a*) J.-E. Bäckvall and A. Gogoll, *J. Chem. Soc., Chem. Commun.*, 1987, 1236–1238; (*b*) E. J. Horn, B. R. Rosen, Y. Chen, J. Tang, K. Chen, M. D. Eastgate and P. S. Baran, *Nature*, 2016, **533**, 77–81; (*c*) Y. Kawamata, M. Yan, Z.-Q. Liu, D.-H. Bao, J.-S. Chen, J. T. Starr and P. S. Baran, *J. Am. Chem. Soc.*, 2017, **139**, 7448–7451; (*d*) Y. Liang, S.-H. Shi, R. Jin, X. Qiu, J. Wei, H. Tan, X. Jiang, X. Shi, S. Song and N. Jiao, *Nat. Catal.*, 2021, **4**, 116–123; (*e*) M. A. Hoque, J. Twilton, J. Zhu, M. D. Graaf, K. C. Harper, E. Tuca, G. A. DiLabio and S. S. Stahl, *J. Am. Chem. Soc.*, 2022, **144**, 15295–15302.

5 (*a*) H. Wang, X. Gao, Z. T. Abdelilah and A. Lei, *Chem. Rev.*, 2019, **119**, 6769–6787; (*b*) J. L. Röckl, D. Pollok, R. Franke and S. R. Waldvogel, *Acc. Chem. Res.*, 2020, **53**, 45–61; (*c*) A. Kirste, G. Schnakenburg, F. Stecker, A. Fischer and S. R. Waldvogel, *Angew. Chem., Int. Ed.*, 2010, **49**, 971–975; (*d*) P. Wang, S. Tang, P. Huang and A. Lei, *Angew. Chem., Int. Ed.*, 2017, **56**, 3009–3013; (*e*) Z.-J. Wu and H.-C. Xu, *Angew. Chem., Int. Ed.*, 2017, **56**, 4734–4738; (*f*) T. J. DeLano and S. E. Reisman, *ACS Catal.*, 2019, **9**, 6751–6754; (*g*) H. Kim, H. Kim, T. H. Lambert and S. Lin, *J. Am. Chem. Soc.*, 2020, **142**, 2087–2092; (*h*) G.-Q. Sun, W. Zhang, L.-L. Liao, L. Li, Z.-H. Nie, J.-G. Wu, Z. Zhang and D.-G. Yu, *Nat. Commun.*, 2021, **12**, 7086; (*i*) W. Zhang, L. Lu, W. Zhang, S. D. Ware, J. Mondragon, J. Rein, N. Strotman, D. Lehnherr, K. A. See and S. Lin, *Nature*, 2022, **604**, 292–297.

6 (*a*) F. Kakiuchi, T. Kochi, H. Mutsutani, N. Kobayashi, S. Urano, M. Sato, S. Nishiyama and T. Tanabe, *J. Am. Chem. Soc.*, 2009, **131**, 11310–11311; (*b*) A. Badalyan and S. S. Stahl, *Nature*, 2016, **535**, 406–410; (*c*) J. Xiang, M. Shang, Y. Kawamata, H. Lundberg, S. H. Reisberg, M. Chen, P. Mykhailiuk, G. Beutner, M. R. Collins, A. Davies, M. Del Bel, G. M. Gallego, J. E. Spangler, J. Starr, S. Yang, D. G. Blackmond and P. S. Baran, *Nature*, 2019, **573**, 398–402; (*d*) T.-J. He, Z.-R. Ye, Z.-F. Ke and J.-M. Huang, *Nat. Commun.*, 2019, **10**, 833; (*e*) Y. Qiu, A. Scheremetjew and L. Ackermann, *J. Am. Chem. Soc.*, 2019, **141**, 2731–2738; (*f*) L. F. T. Novaes, J. S. K. Ho, K. Mao, K. Liu, M. Tanwar, M. Neurock, E. Villemure, J. A. Terrett and S. Lin, *J. Am. Chem. Soc.*, 2022, **144**, 1187–1197; (*g*) C. Huang, W. Ma, X. Zheng, M. Xu, X. Qi and Q. Lu, *J. Am. Chem. Soc.*, 2022, **144**, 1389–1395; (*h*) J. Zhang, B. Das, O. Verho and J.-E. Bäckvall, *Angew. Chem., Int. Ed.*, 2022, **61**, e202212131; (*i*) L.-H. Jie, B. Guo, J. Song and H.-C. Xu, *J. Am. Chem. Soc.*, 2022, **144**, 2343–2350; (*j*) L.-L. Liao, Z.-H. Wang, K.-G. Cao, G.-Q. Sun, W. Zhang, C.-K. Ran, Y. Li, L. Chen, G.-M. Cao and D.-G. Yu, *J. Am. Chem. Soc.*, 2022, **144**, 2062–2068.

7 (*a*) M. Rafiee, F. Wang, D. P. Hruszkewycz and S. S. Stahl, *J. Am. Chem. Soc.*, 2018, **140**, 22–25; (*b*) Z.-W. Hou, D.-J. Liu, P. Xiong, X.-L. Lai, J.-S. Song and H.-C. Xu, *Angew. Chem., Int. Ed.*, 2021, **60**, 2943–2947; (*c*) Z. Ruan, Z. Huang, Z. Xu, S. Zeng, P. Feng and P.-H. Sun, *Sci. China: Chem.*, 2021, **64**, 800–807; (*d*) M. Stangier, A. Scheremetjew and L. Ackermann, *Chem. – Eur. J.*, 2022, **28**, e202201654.

8 S. R. Waldvogel and M. Selt, *Angew. Chem., Int. Ed.*, 2016, **55**, 12578–12580.

9 (*a*) F. Wang, M. Rafiee and S. S. Stahl, *Angew. Chem., Int. Ed.*, 2018, **57**, 6686–6690; (*b*) Z.-H. Wang, P.-S. Gao, X. Wang, J.-Q. Gao, X.-T. Xu, Z. He, C. Ma and T.-S. Mei, *J. Am. Chem. Soc.*, 2021, **143**, 15599–15605; (*c*) H. Wang, M. He, Y. Li, H. Zhang, D. Yang, M. Nagasaka, Z. Lv, Z. Guan, Y. Cao, F. Gong, Z. Zhou, J. Zhu, S. Samanta, A. D. Chowdhury and A. Lei, *J. Am. Chem. Soc.*, 2021, **143**, 3628–3637.

10 T. Shono, H. Hamaguchi and Y. Matsumura, *J. Am. Chem. Soc.*, 1975, **97**, 4264–4268.

11 (*a*) Y. Takahira, M. Chen, Y. Kawamata, P. Mykhailiuk, H. Nakamura, B. K. Peters, S. H. Reisberg, C. Li, L. Chen, T. Hoshikawa, T. Shibuguchi and P. S. Baran, *Synlett*, 2019, 1178–1182; (*b*) Y. Liu, B. Shi, Z. Liu, R. Gao, C. Huang, H. Alhumade, S. Wang, X. Qi and A. Lei, *J. Am. Chem. Soc.*, 2021, **143**, 20863–20872; (*c*) L. Zhang, Y. Fu, Y. Shen, C. Liu,

 This journal is © The Royal Society of Chemistry 2023

Published on 09 maart 2023. Downloaded on 13/10/2025 18:40:56.

M. Sun, R. Cheng, W. Zhu, X. Qian, Y. Ma and J. Ye, *Nat. Commun.*, 2022, **13**, 4138.

12 (*a*) G.-Q. Xu, J.-T. Xu, Z.-T. Feng, H. Liang, Z.-Y. Wang, Y. Qin and P.-F. Xu, *Angew. Chem., Int. Ed.*, 2018, **57**, 5110–5114; (*b*) X. Shi, Y. He, X. Zhang and X. Fan, *Adv. Synth. Catal.*, 2018, **360**, 261–266; (*c*) A. F. Prusinowski, R. K. Twumasi, E. A. Wappes and D. A. Nagib, *J. Am. Chem. Soc.*, 2020, **142**, 5429–5438; (*d*) W. Chen, A. Paul, K. A. Abboud and D. Seidel, *Nat. Chem.*, 2020, **12**, 545–550; (*e*) D. A. Valles, S. Dutta, A. Paul, K. A. Abboud, I. Ghiviriga and D. Seidel, *Org. Lett.*, 2021, **23**, 6367–6371; (*f*) X. Liu, Z. Wang, Q. Wang and Y. Wang, *Angew. Chem., Int. Ed.*, 2022, **61**, e202205493.

13 T. Shen and T. H. Lambert, *Science*, 2021, **371**, 620–626.

14 (*a*) L. Buglioni, F. Raymenants, A. Slattery, S. D. A. Zondag and T. Noël, *Chem. Rev.*, 2022, **122**, 2752–2906; (*b*) J. P. Barham and B. König, *Angew. Chem., Int. Ed.*, 2020, **59**, 11732–11747; (*c*) S. Wu, J. Kaur, T. A. Karl, X. Tian and J. P. Barham, *Angew. Chem., Int. Ed.*, 2022, **61**, e202114672.

15 T. Shen, Y.-L. Li, K.-Y. Ye and T. H. Lambert, *Nature*, 2023, **614**, 275–280.

16 (*a*) T. Feng, S. Wang, Y. Liu, S. Liu and Y. Qiu, *Angew. Chem., Int. Ed.*, 2022, **61**, e202115178; (*b*) T. Feng, S. Wang and Y. Qiu, *Synlett*, 2022, 1582–1588.

17 (*a*) P. Li, C. Guo, S. Wang, D. Ma, T. Feng, Y. Wang and Y. Qiu, *Nat. Commun.*, 2022, **13**, 3774; (*b*) Y. Wang, S. Tang, G. Yang, S. Wang, D. Ma and Y. Qiu, *Angew. Chem., Int. Ed.*, 2022, **61**, e202207746; (*c*) Y. Wang, Z. Zhao, D. Pan, S. Wang, K. Jia, D. Ma, G. Yang, X.-S. Xue and Y. Qiu, *Angew. Chem., Int. Ed.*, 2022, **61**, e202210201; (*d*) Z. Zhao, Y. Liu, S. Wang, S. Tang, D. Ma, Z. Zhu, C. Guo and Y. Qiu, *Angew. Chem., Int. Ed.*, 2023, **62**, e202214710; (*e*) S. Wang, T. Feng, Y. Wang and Y. Qiu, *Chem. - Asian J.*, 2022, **17**, e202200543.

18 R. D. Jana, D. Sheet, S. Chatterjee and T. K. Paine, *Inorg. Chem.*, 2018, **57**, 8769–8777.

19 D. Gunasekera, J. P. Mahajan, Y. Wanzi, S. Rodrigo, W. Liu, T. Tan and L. Luo, *J. Am. Chem. Soc.*, 2022, **144**, 9874–9882.

20 (*a*) U. Karst, *Angew. Chem., Int. Ed.*, 2004, **43**, 2476–2478; (*b*) M. Lu, Y. Liu, R. Helmy, G. E. Martin, H. D. Dewald and H. Chen, *J. Am. Soc. Mass Spectrom.*, 2015, **26**, 1676–1685; (*c*) C. Mu, W. Wang, J. Wang, C. Gong, D. Zhang and X. Zhang, *Angew. Chem., Int. Ed.*, 2020, **59**, 21515–21519.